Experimental Report

Proposal: **5-24-423** **Council:** 4/2010

Title: High pressure study of ammonia monohydrate from 0 — 3.0 GPa

This proposal is a new proposal

Researh Area: Materials

Main proposer: **FORTES Andrew Dominic**

Experimental Team: SCLATER Gillian
FORTES Andrew Dominic
NORMAN Lucy
KOLB Mathis
NAUMANN Nicolas

Local Contact: HANSEN Thomas

Samples: Ammonia monohydrate-d5 (ND3.D2O)

Instrument	Req. Days	All. Days	From	To
D20	6	6	09/12/2010	15/12/2010

Abstract:

Ammonia monohydrate, exists in at least six different crystalline phases under varying conditions of pressure and temperature. Hitherto, only the structures of the lowest pressure phase (AMH I, P212121) and highest pressure phase (AMH VI, Im-3m) were known; we have since determined the structure of one other high-P phase (AMH II, Pbca). Our objective here is to collect high resolution powder data from AMH phases III, IV, and V, in order to determine their crystal structures. We will combine our previously successful blend of ab initio computational structure prediction, and powder structure determination, which was used to obtain the AMH II structure. We will also obtain new data on the thermoelastic properties of AMH phases II and III, whilst also constraining solid-solid and solid-liquid phase boundaries of the other polymorphs.

High pressure study of ammonia monohydrate

Introduction

Ammonia monohydrate, $NH_3 \cdot H_2O$ (hereafter AMH) is known to exist as at least six different crystalline polymorphs under varying conditions of pressure and temperature up to ~ 6 GPa; Much of our knowledge concerning the high-pressure polymorphism has come from experiments carried out by Richard Nelmes' group using the Paris-Edinburgh cell at ISIS in the late nineties. Although preliminary data from these experiments were published [*1,2*], few of the observations have been reproduced independently (although all but one of the reported phases was observed in two separate samples), and the group has solved only the structure of the highest-pressure polymorph, AMH VI, which is a disordered body-centred cubic phase [*3*].

Our group is working on AMH for two reasons. Firstly, both ammonia dihydrate and ammonia monohydrate are candidate 'rock-forming' minerals expected to be abundant in the outer solar system; their behaviour at high-pressures is therefore relevant to geophysical modeling of icy satellite interiors. Furthermore, ammonia dihydrate is known to become unstable at high-pressure, breaking down to AMH + ice [*4*]. Secondly, we have been using computational methods to predict crystal structures [*5,6*]. In the context of this study, we predicted the correct structure of AMH II using only the unit-cell dimensions supplied from the powder-pattern indexing of Fortes *et al*. [*7*]. This structure was confirmed using powder data collected on D2B [*8,9*].

In support of both of these activities, we proposed to collect powder data from ammonia monohydrate polymorphs using the Paris-Edinburgh cell on D20; the results of our initial investigation are presented below.

Sample preparation and loading

Two loadings of the Paris-Edinburgh cell were carried out during our allocated beam-time. The first was devoted to gaining familiarity with the method of loading a volatile specimen into nitrogen cooled gaskets, and assembling the press and its associated cryostat heat shields; an aqueous ammonia liquid corresponding to the dihydrate composition was selected for this test loading, since it is easier to handle. During our first day on D20, we successfully loaded and crystallized this specimen, collecting an excellent powder pattern from the phase we have previously identified as ADH IV [*7*]. However, we discovered that the rolled Pb foils we use as a pressure calibrant were invisible in the diffraction data if not supported in the centre of the gasket space. The second loading utilized an aqueous ammonia liquid corresponding to the monohydrate composition (1:1 ND_3:D_2O). Learning from our previous loading, we prepared a small lead coil by wrapping a shaving from a Pb brick around the tip of a pair of tweezers; this provided an excellent signal in the diffracted beam (Figure 3).

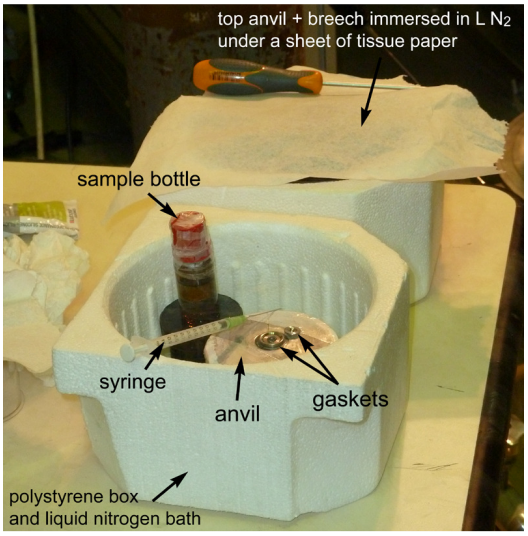

Figure 1: Loading the specimen using nitrogen-cooled anvils and gaskets proved to be very straightforward and quick.

Both anvils were partially immersed in liquid nitrogen inside polystyrene boxes (Figure 1); boiled off dry N_2 gas in the top of each box prevented significant icing from occurring on the anvils or gaskets. The specimen itself and the syringe used to dispense it were stored in the cold N_2 boil-off. This arrangement kept the specimen below its boiling point throughout the loading process. Droplets of AMH liquid were dispensed into the top and bottom gasket cups, where they froze quickly. The upper cup was inverted and pressed down onto the bottom cup with pressure from a pair of warm tweezers. The cold anvil bearing the gaskets was placed into the P-E press, and the cold top anvil+breech was screwed down onto the gaskets; a load of 70 bars was applied to the hydraulic ram, sealing the system, after which the system warmed up to room temperature during assembly of the cryostat heat shields.

Compression of AMH

Figure 2 shows the P-T path followed during loading 2, using the AMH specimen. The data acquired during this time is summarized in Figure 3. Once mounted on the D20 sample stage, neutron powder diffraction data were collected using the 90° take-off port, viewing the 113 plane of the germanium monochromator (λ = 2.41 Å). This combination of wavelength and take-off proved to be ideal for the planned observations. The initial diffraction pattern, acquired under 70 bar load at room-T, showed a broad amorphous feature around 2θ = 45° from the liquid AMH specimen, and four sharp strong Bragg reflections from the Pb pressure marker. Cooling to 170 K and slowly

High pressure study of ammonia monohydrate

increasing the load to 250 bars caused the specimen to crystallize – marked **(1)** on Figures 2 and 3. The positions of the observed reflections match those of the orthorhombic low-pressure phase AMH I ($P2_12_12_1$); however, the intensities differ significantly from the calculated values, and a number appear to be absent altogether, from which we conclude that the specimen initially formed a single crystal of AMH I rather than a powder.

Weak parasitic peaks from AMH II grew over ~2 hours, and upon increasing the load to 260 bar became dominant. This phase-pure AMH II powder specimen was then compressed in 20 bar increments (each ~1.2 kbar on the specimen) along the 180 K isotherm – marked **(2)** in Figures 2 and 3. Diffraction data were integrated for 80 minutes at each datum, from which we were able to refine the unit-cell parameters of AMH II to high precision. These data yield the equation of state of AMH II over the range 4 – 25 kbar; previously we could access only the range 4-5 kbar using a gas pressure vessel. We find that the *c*-axis of AMH II is the most compressible, and the *b*-axis the least compressible; the *a*-axis falls mid-way between the two extremes. A Murnaghan equation of state fitted to the unit-cell volumes as a function of pressure yields the zero-pressure volume, V_0 = 947(2) Å^3, the zero-pressure incompressibility, K_0 = 7.2(3) GPa, and its first pressure derivative $\partial K_0/\partial T$ = 5.3(2).

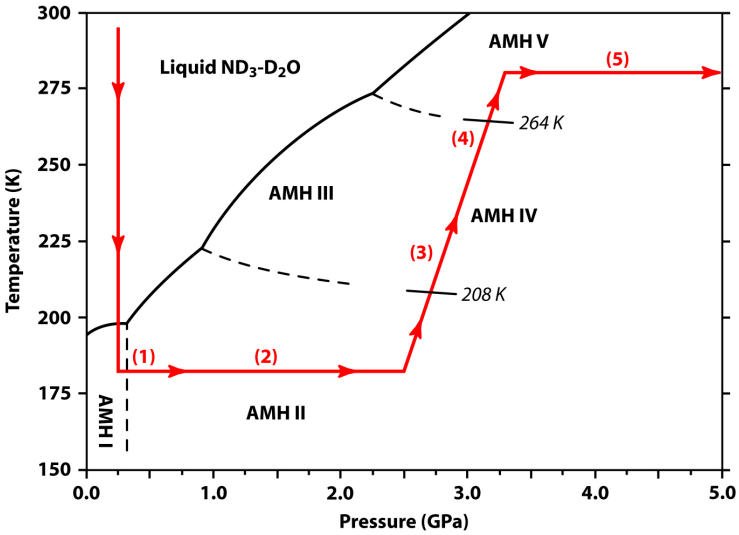

Figure 2: The P-T phase diagram of AMH, showing the inflected melting curve first proposed by Kargel and Hogenboom [*10*], and plausible solid-solid transitions (dashed lines) that are consistent with all published observations [*1,2,10*]. Our path through the phase diagram is marked by the solid red line; numbers refer to the panels in Figure 3, and the solid black lines (with temperatures appended) indicate where phase transitions were observed upon warming.

Although we anticipated a phase transition from AMH II → IV around 2–2.25 GPa at 180 K [*1,2*], this was not observed. At a load of 620 bars (~2.5 GPa), we commenced a slow warming ramp from 180 K → 250 K (approx. 0.1 K min^{-1}) – marked **(3)** on Figures 2 and 3. A phase transition was observed upon warming through 208 K. The diffraction pattern of this new phase does not match the patterns reported previously for either AMH III or IV, although the published patterns of either are not well suited for making such a comparison. However, the shift of the main cluster of strong Bragg reflections to higher angles better matches the pattern of AMH IV, and is crudely interpreted as indicating a volume decrease of ~ 10 %. We integrated data from this phase, which *may* be AMH IV, for 4 hours at 250 K.

Warming was continued, under a load of 620 bars, from 250 K → 280 K – marked **(4)** on Figures 2 and 3. Another phase transition was observed at 264 K to a phase which is recognizable from earlier work as AMH Vb. Since we doubt that AMH Va and Vb are truly different AMH phases (it is plausible that phase Va is simply Vb with an impurity), we will only refer to this phase as AMH V. Data were integrated from AMH V for 6 hours at 280 K. Subsequently, AMH V was compressed in 20 bar steps from 620 → 1000 bars, and in 50 bar steps thereafter, up to a final load of 1350 bar (~ 8 GPa) – marked **(5)** on Figures 2 and 3. No phase transition to the bcc phase AMH VI [*3*] was observed even at the highest applied load.

Summary

We have successfully synthesized and collected data from four AMH polymorphs. Although efforts to index AMH IV (?) and AMH V continue, we have narrowly defined their phase boundaries with one another, and between phases II and IV. We have measured the equation of state over a range twenty times larger than was previously accessible to us in the gas cell. We also have the data necessary to fit an equation of state for AMH V over the range 3.25 – 8 GPa once this phase is indexed. The decision to devote a day to a test loading and data collection paid off in terms of the quantity and quality of data we subsequently collected from the AMH specimen. Whilst we did not then have time to carry out a second AMH loading in order to synthesize AMH III, we will propose to do this in future. The superb dataset collected on D20 provides us with the basis to develop and test structural models of AMH IV and V using computational prediction methods.

High pressure study of ammonia monohydrate

Figure 3: Summary of all the data collected during the experiment (central panels – numbers correspond to legs of the P-T path in Figure 2), showing shift and changes in Bragg peaks over the range 2θ = 5–115° as a function of instrument run number; each run ≈ 10 minutes. Panels at left and right show the best diffraction patterns of each phase observed (i.e., the longest integrations over tens of 10 minute runs). Red tick marks show the position of the reflections from the Pb pressure marker.

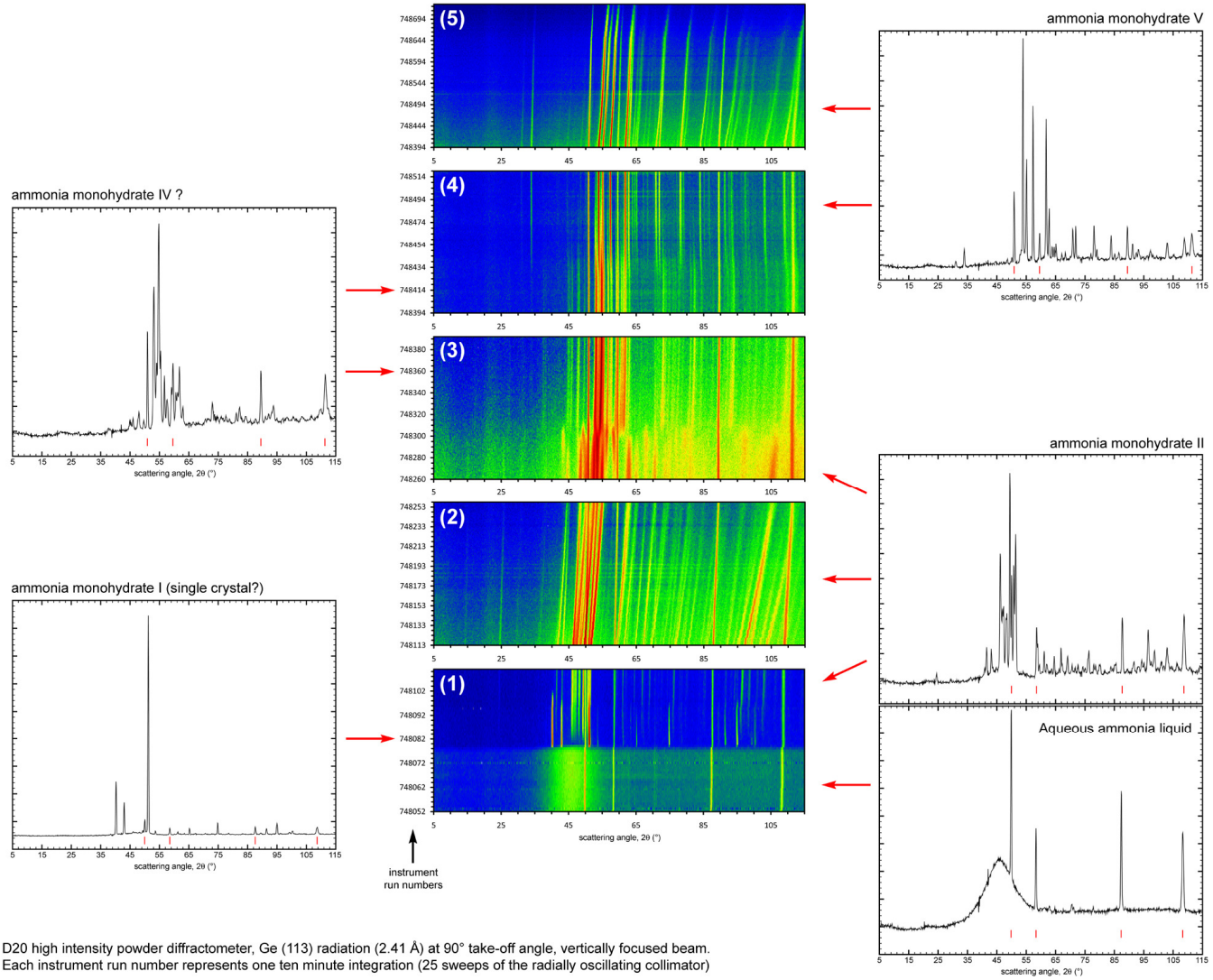

D20 high intensity powder diffractometer, Ge (113) radiation (2.41 Å) at 90° take-off angle, vertically focused beam.
Each instrument run number represents one ten minute integration (25 sweeps of the radially oscillating collimator)

References

[1] Loveday & Nelmes (2000): In *Science and Technology of High Pressure: Proceedings of AIRAPT-17.* pp. 133–136.
[2] Loveday & Nelmes (2004) *High Press. Res.* **24**(1), 45-55.
[3] Loveday & Nelmes (1999): *Phys. Rev. Lett.* **83**, 4329-4332.
[4] Fortes *et al.* (2007): *High Press. Res.* **27**(2), 201-212.
[5] Pickard & Needs (2006): *Phys. Rev. Lett.* **97**, article 045504.
[6] Pickard & Needs (2008): *Nature Materials* **7**, 775-779.
[7] Fortes *et al.* (2009a): *J. Appl. Cryst.* **42**(5), 846-866.
[8] Fortes *et al.* (2009b): *J. Am. Chem. Soc.* **131**(37), 13508-13515.
[9] Fortes *et al.* (2009c): *J. Chem. Phys.* **131**(15), article 154503.
[10] Kargel & Hogenboom (1995): *Lunar Planet. Sci.* **26**, 725-726.